

***E0* transitions in deformed nuclei**Gabriela Ilie<sup>1,2</sup> and Richard F. Casten<sup>1</sup><sup>1</sup>*Wright Nuclear Structure Laboratory, Yale University, New Haven, Connecticut 06520, USA*<sup>2</sup>*National Institute for Physics and Nuclear Engineering, P.O. Box MG-6, Bucharest-Măgurele, Romania*

(Received 1 November 2011; published 22 December 2011)

*E0* transitions are a sensitive indicator of structure in nuclei, reflecting shape transitional regions, deformation, and intruder states. Attention has generally focused on *E0* transitions to the ground state or low-lying yrast levels. In this paper we look at all *E0* transitions connecting  $0^+$  states in a rather general collective model. We deduce a new selection rule and map out calculated strengths throughout the spectrum. The distributions of *E0* strengths for several different collective structures are discussed.

DOI: [10.1103/PhysRevC.84.064320](https://doi.org/10.1103/PhysRevC.84.064320)

PACS number(s): 21.60.Ev, 21.10.Re, 21.10.Ky

**I. INTRODUCTION**

Though less studied than electric quadrupole transitions, *E0* transitions are a sensitive signature of structure. There have been a number of theoretical treatments of these transitions. Although a consensus on their interpretation has sometimes been lacking [1–4], it is clear that they are particularly sensitive to changes in nuclear shape, growing rapidly in strength in spherical-deformed shape/phase transition regions. They have been predicted, in the context of the interacting boson approximation (IBA) model [5], to remain large throughout the deformed region [4]. A recent study using a geometric model [6] has investigated their behavior as a function of the stiffness of the quadrupole potential. In addition, their correlation with nuclear radii has been investigated in Ref. [7]. In some models, such as the IBA model, there are definite selection rules and analytic predictions for the strengths of *E0* transitions from excited  $0^+$  state to the ground state in the cases of the dynamical symmetries. In recent years there have been attempts [8] to test these predictions in deformed nuclei but such tests are experimentally difficult, primarily because, in a perfect rotor, the energies of successive *E0* transitions to the yrast states, that is, transitions of the form  $J \rightarrow J$  (yrast) have identical energies.

Our aim here is to use the IBA model to map out the full spectrum of  $0^+ \rightarrow 0^+$  *E0* transitions for several different structural situations. We start with the dynamical symmetries O(6) and SU(3) [all *E0* transitions are identically zero in U(5)] and then look at cases in the interior of the symmetry triangle of the IBA, including a calculation along the arc of regularity [9]. We will do the calculations for different numbers of valence nucleons to check for consistency of the results. In the case of a well-deformed rotor of SU(3) type, we will show the existence of a new selection rule that simultaneously describes all the allowed  $0^+ \rightarrow 0^+$  *E0* transitions and we will study the breakdown of that selection rule for deformed nuclei deviating from a pure SU(3) structure.

Although *E0* transitions present experimental challenges, these results should be useful for studying the correlations with structure that they show. These correlations are related to issues of order and chaos, for vividly highlighting the breakdown of the dynamical symmetries, for showing the interrelationships of excited  $0^+$  states (the *E0* operator in the IBA is directly

related to the *s*- and *d*-boson structure of the states), and for again pointing to the uniqueness of the arc of regularity.

**II. SELECTION RULES FOR *E0* TRANSITIONS**

In the IBA model there are three dynamical symmetries characterized by analytic expressions for eigenvalues and transition rates and a number of selection rules for these limiting cases. Even though very few nuclei actually exhibit the strict constraints of these symmetries, these analytic relations are useful as benchmarks (analogously to the role of magic numbers in the shell model) to which realistic calculations that break the symmetries can be compared.

To this end, Table I gives the selection rules for *E0* transitions to the ground state that have been deduced [5] for U(5)—analogous to a spherical vibrator, SU(3)—a specific form of the axial deformed rotor, and O(6)—corresponding to a  $\gamma$ -soft axially symmetric rotor.

These are highly restrictive, allowing a single *E0*  $0^+ \rightarrow 0^+$  transition in the SU(3) and O(6) cases and none in U(5). However, they say nothing about *E0* transitions between higher lying  $0^+$  states, which is the main interest of this study. Figure 1 illustrates the three dynamical symmetries of the IBA in terms of the symmetry triangle and the allowed *E0* transitions to the ground state for the SU(3) and the O(6) symmetries. The lowest excited  $0^+$  states in each corner of the triangle for U(5), SU(3), and O(6) are labeled with their quantum numbers,  $n_d$  for U(5),  $(\lambda, \mu)$  for SU(3) and  $(\sigma, \tau)$  for O(6) where  $N$  in the SU(3) and O(6) cases is the total number of bosons. The red and green dots in Fig. 1 correspond to calculations of the *E0* transitions inside the symmetry triangle of the IBA on the arc of regularity and near the middle of the triangle, respectively. For each corner the ratio between the energies of the first excited  $4^+$  and  $2^+$  states,  $R_{4/2}$  is given.

The question we want to address is to look at all  $0^+ \rightarrow 0^+$  transitions in these limits and between them as well. To do this, we use the standard IBA Hamiltonian

$$H = \varepsilon n_d + \kappa Q \cdot Q \quad (1)$$

with  $Q = s^\dagger \tilde{d} + d^\dagger s + \chi [d^\dagger \tilde{d}]^{(2)}$ .

The three symmetry limits are obtained with particular choices of the coefficients of the terms in the Hamiltonian

TABLE I. Selection rules for ground state  $E0$  transitions in the three dynamical symmetries of the IBA.

Dynamical Symmetry Analogue	Geometric	Essential quantum numbers	$E0$ selection rule	Ground state quantum numbers
U(5)	Spherical vibrator	$n_d$	All forbidden	$n_d = 0$
SU(3)	Axial rotor	$(\lambda, \mu)$	$(\Delta\lambda, \Delta\mu) = (4, 2)$	$(2N, 0)$
O(6)	$\gamma$ soft rotor	$(\sigma, \tau)$	$(\Delta\sigma, \Delta\tau) = (2, 0)$	$(N, 0)$

and of  $\chi$ . For U(5),  $\kappa = 0$  and  $\chi$  therefore is irrelevant. For SU(3),  $\varepsilon = 0$  and  $\chi = -\sqrt{7}/2$ . For O(6),  $\varepsilon = 0$  and  $\chi = 0$ .

Calculations deviating from the symmetries are obtained for intermediate values of the parameters of the Hamiltonian. The Hamiltonian basically represents a competition between a spherical-driving  $n_d$  term and a deformation-driving  $Q \cdot Q$  term. Hence, the structure is given simply by two parameters,  $\varepsilon/\kappa$ , which determines the spherical-deformed nature of the solutions, and  $\chi$ , which controls the  $\gamma$  softness. Since  $\varepsilon/\kappa$  can vary from zero to infinity it is convenient to rewrite the Hamiltonian of Eq. (1) as follows:

$$H(\zeta, \chi) = a \left[ (1 - \zeta)n_d - \frac{\zeta}{4N} Q \cdot Q \right], \quad (2)$$

where  $a$  is a scaling factor. The parametrization of the two Hamiltonian Eqs. (1) and (2) are related by the equation

$$\frac{\varepsilon}{\kappa} = 4N \frac{1 - \zeta}{\zeta}. \quad (3)$$

Thus  $\zeta = 0$  corresponds to U(5) while  $\zeta = 1$  gives SU(3) for  $\chi = -\sqrt{7}/2$  and O(6) for  $\chi = 0$ .  $\zeta$  corresponds to a radius vector in the symmetry triangle from the U(5) vertex toward the O(6)–SU(3) leg, while  $\chi$  corresponds to the angle of this vector of the U(5) to SU(3) leg.

The  $E0$  operator given by [5]:

$$T_0^{(E0)} = \alpha [s^\dagger s]_0^{(0)} + \beta [d^\dagger \tilde{d}]_0^{(0)} \quad (4)$$

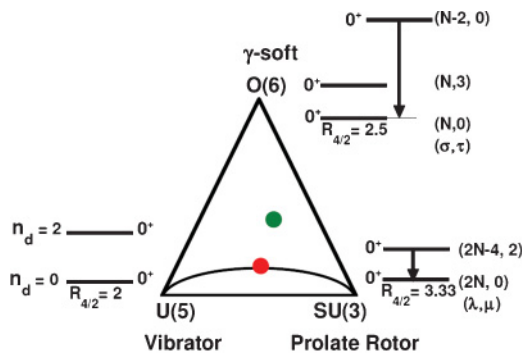


FIG. 1. (Color online) Symmetry triangle of the IBA model giving the three limiting symmetries and the Alhassid-Whelan arc of regularity. For each symmetry, the allowed transitions between the first excited  $0^+$  state and the ground state are shown. The level schemes are labeled by their quantum numbers. The two dots inside the triangle represent calculations for  $E0$  transitions between all excited states for a point on the arc of regularity (red dot) and near the middle of the triangle (green dot).

can be rewritten in terms of the total boson number  $N = n_s + n_d$  as

$$T_0^{(E0)} = \alpha N + \beta' [d^\dagger \tilde{d}]_0^{(0)} \quad (5)$$

with  $\beta' = \beta - \alpha\sqrt{5}$ . The constant term  $\alpha N$  does not give rise to electromagnetic transitions. Thus one needs to evaluate the matrix elements of the last operator in Eq. (5).

### III. RESULTS FOR THE THREE DYNAMICAL SYMMETRIES

Since  $n_d$  is a good quantum number for U(5) there are no allowed  $E0$  transitions in that limit. For all other calculations, it is easy to evaluate this transition strength numerically since the standard IBA code expands the wave functions in  $n_d$ . The results will depend on the total boson number,  $N$ . We will show the results for SU(3) and O(6) in two forms: in terms of a symmetric matrix of  $\rho^2(E0)$  values where the columns and rows are labeled by their quantum numbers, and pictorially in terms of a level scheme diagram of the ground and excited  $0^+$  states and the allowed transitions between them. Figure 2 shows the results for O(6) nuclei for  $N = 6$  bosons. Figure 3 shows similar results for SU(3) symmetry for  $N = 16$  bosons.

Turning to Fig. 2, we see that some levels [such as the first excited  $0^+$  state, with  $(\sigma, \tau) = (N, 3)$ ] have no allowed  $E0$  decays. Those states with the same  $\tau$  but different  $\sigma$  have only a single allowed transition. That is, the selection rule for ground state transitions actually persists for all  $0^+ \rightarrow 0^+$   $E0$  transitions and, for a state with a given  $(\sigma, \tau)$ , there is at most only one lower lying level satisfying it.

For SU(3), this is not the case as Fig. 3 shows. Here all  $0^+$  levels have at least one allowed decay and some have several (but not many—see below). Even just the decay of the third excited  $0^+$  state shows that the simple selection rule for SU(3) in Table I is not adequate to describe the  $E0$  transitions from the higher states. Using the matrices in Fig. 3, we have found a heretofore unrecognized selection rule that describes all allowed  $0^+ \rightarrow 0^+$   $E0$  transitions in SU(3). This rule can be expressed in two ways. In the usual notation of  $(\lambda, \mu)$  quantum numbers  $0^+ \rightarrow 0^+$   $E0$  transitions are allowed if any of the following three conditions is satisfied:

$$(\Delta\lambda, \Delta\mu) = (2, 4), (2, 2), (4, 2). \quad (6)$$

These rules are sufficient albeit awkward. However, with a different notation, using Young Tableaux (for an excellent elementary discussion of Young Tableaux, see [10]), it is easy to express these three results by a single simple rule.

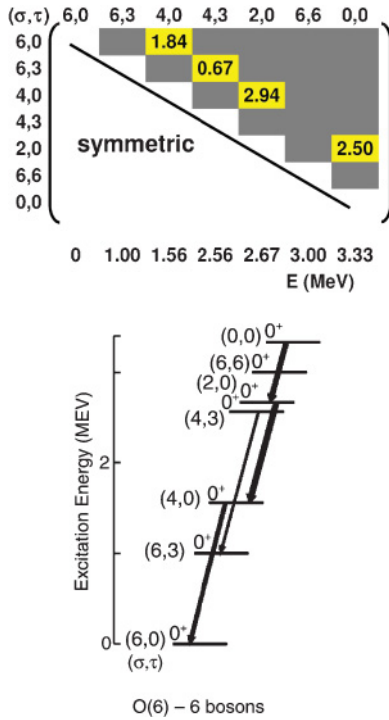


FIG. 2. (Color online) Calculated  $E0$  transition strengths (arbitrary units) for the  $O(6)$  limit for  $N = 6$  bosons. Top panel: The  $E0$  matrix elements  $\rho^2(E0, J_i \rightarrow J_f)$  predicted by the IBA are shown. The corresponding  $O(6)$  quantum numbers  $(\sigma, \tau)$  are also given in the figure. The energies are normalized to the first excited  $0^+$  state. Bottom panel: All  $E0$  transitions between all  $0^+$  levels are shown. In this and the next two figures the thickness of the arrows give a indication of the  $\rho^2(E0)$  strengths.

Figure 4 (upper part) shows the Young Tableaux representation for  $SU(3)$  symmetry described in terms of two rows of boxes. The difference in the number of boxes between the second and first rows gives  $\lambda$ , while  $\mu$  is given by the number of boxes in the second row. Manipulating the boxes between the two rows according to the rules in Eq. (6) gives the  $SU(3)$  representations that are connected by allowed  $E0$  transitions. The Young Tableaux designations for  $SU(3)$  in Fig. 4 (top) are equivalent to a scheme with three rows, as shown in the bottom of the figure. Here, the number of boxes in the successive rows are given by  $n_1, n_2, n_3$ . The rows are ordered such that their length always decreases as the row number increases,  $n_1 > n_2 > n_3$ . Here,  $\lambda$  is again given by the difference in the number of boxes between the second and first rows, while  $\mu$  is the difference in the number of boxes between the second and third rows. In effect, one obtains the upper description of  $SU(3)$  in Fig. 4 by truncating the boxes on the left in which all rows are occupied. In the lower part of Fig. 4, the ground state can be represented by a single row of  $2N$  boxes and has  $(\lambda, \mu) = (2N, 0)$ . The next representation is formed by moving two boxes into the second row giving  $(\lambda, \mu) = (2N - 4, 2)$ . Two additional boxes can be moved from the upper row to either the second or third rows, resulting in, respectively,  $(\lambda, \mu) = (2N - 8, 4)$  or  $(2N - 6, 0)$ , and so on.

TABLE II. Selection rules for  $E0$  transitions of the  $SU(3)$  symmetry, for  $N = 12$  bosons, in terms of Young diagrams with three rows. The  $n_1, n_2, n_3$  represent the numbers of boxes in the first, middle and third rows of Young diagram and  $(\lambda, \mu)_{i,f}$  are the initial and final quantum numbers.

$(\lambda, \mu)_i \equiv (n_1, n_2, n_3)$	$(\lambda, \mu)_f \equiv (n_1, n_2, n_3)$	$(\Delta\lambda, \Delta\mu)$
$(16, 4) \equiv (20, 4, 0)$	$(14, 2) \equiv (18, 4, 2)$	$(2, 2)$
$(16, 4) \equiv (20, 4, 0)$	$(12, 6) \equiv (18, 6, 0)$	$(4, 2)$
$(16, 4) \equiv (20, 4, 0)$	$(18, 0) \equiv (20, 2, 2)$	$(2, 4)$
$(16, 4) \equiv (20, 4, 0)$	$(24, 0) \equiv (24, 0, 0)$	forbidden

In this notation, all allowed  $E0$  transitions in  $SU(3)$  can be described by the following rule: any transition connecting two  $0^+$  states is allowed if the Young Tableaux for either state can be converted into that for the other state by taking two boxes from a higher row to any lower row. This can be from  $n_1$  to  $n_2$ , or  $n_1$  to  $n_3$ , or  $n_2$  to  $n_3$ . That is, two states are connected if

$$\Delta n_i = n_j \pm 2 \quad \text{for } i \neq j \quad (7)$$

with the third row unchanged.

We illustrate the selection rules with one example. Consider the allowed transition in  $SU(3)$  for 12 bosons from the state  $(16, 4)$  to  $(14, 2)$ . This is  $(\Delta\lambda, \Delta\mu) = (2, 2)$ . In terms of the Young Tableaux with three rows this is a movement of two boxes from  $n_1$  to  $n_3$ . For the same number of bosons in  $SU(3)$  if we consider the transition from the state  $(16, 4)$  to  $(12, 6)$ , this is  $(\Delta\lambda, \Delta\mu) = (4, 2)$ . In terms of the Young Tableaux with three rows this is a movement of two boxes from  $n_1$  to  $n_2$ . In the case of the transition  $(18, 0)$  to  $(16, 4)$ , this is  $(\Delta\lambda, \Delta\mu) = (2, 4)$ . In terms of the Young Tableaux with three rows this is a movement of two boxes from  $n_2$  to  $n_3$ . If we consider the transition from state  $(16, 4)$  to  $(24, 0)$ , this is  $(\Delta\lambda, \Delta\mu) = (8, 4)$  which is forbidden according to the rules in Eq. (6) and by the Young Tableaux representation with three rows. These results are summarized in Table II.

With this result in hand, and the ones for  $U(5)$  and  $O(6)$ , we can now study how the  $E0$  strengths and their distributions vary for nuclei with structures corresponding to interior positions in the triangle.

#### IV. RESULTS FOR NUCLEI DEVIATING FROM THE DYNAMICAL SYMMETRIES

The simple  $E0$  decay patterns seen in Figs. 2 and 3 reflect the character of the symmetries and the existence of good numbers at the vertices of the triangle. Away from those vertices, mixing of the states of the symmetries occurs such that the quantum numbers rapidly lose validity and, generally, a larger number of  $E0$  transitions have finite values. We illustrate this with two calculations, one for the special case of nuclei along the arc of regularity and one for a typical deformed nucleus.

Figure 5 shows the level scheme and  $E0$  transitions for two calculations with parameters corresponding to the positions marked by the colored dots in Fig. 1, along with the results for  $SU(3)$  for comparison. The case in the middle of Fig. 5

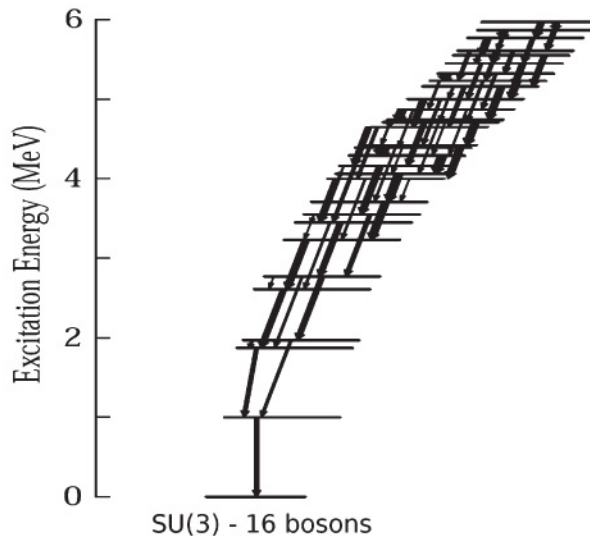
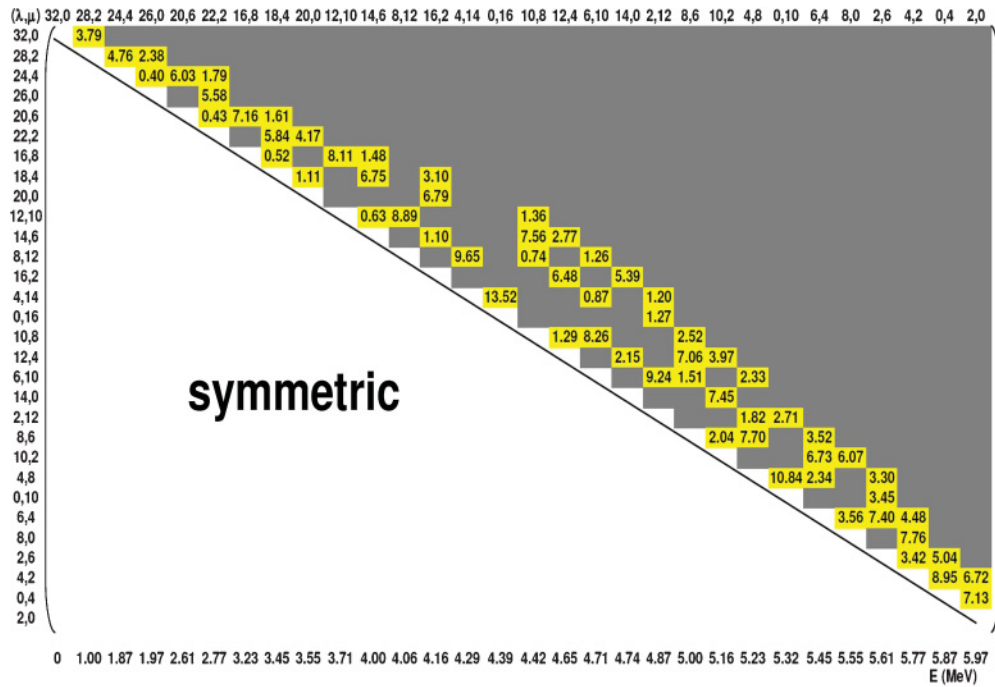


FIG. 3. (Color online) Calculated  $E0$  transition strengths (arbitrary units) for the  $SU(3)$  limit for  $N = 16$  bosons. Top panel: The  $E0$  matrix elements  $\rho^2(E0, J_i \rightarrow J_f)$  predicted by the IBA are shown. The corresponding  $SU(3)$  quantum numbers  $(\lambda, \mu)$  are also given in the figure. The energies are normalized to the first excited  $0^+$  state. Bottom panel: All  $E0$  transitions between all  $0^+$  levels are shown.

corresponds to a deformed nucleus lying along the arc of regularity (red dot). The arc is a unique region, discovered by Alhassid and Whelan [9] about twenty years ago where, amidst nuclei whose properties appear to be highly chaotic, there is a narrow valley of regularity starting at  $SU(3)$  and heading toward the spherical-deformed phase transitional line and then beyond toward  $U(5)$ . In this valley, despite the distance from  $SU(3)$ , the spectra regain ordered behavior. For years it was thought that this region was of only academic interest since it was devoid of actual nuclei. However, about a decade ago, new fits of the IBA [4] identified a set of eight well-deformed nuclei that lie very close to the arc. A common characteristic was noted, namely the near degeneracy of the first excited  $0^+$  state

and the  $2^+$  level of its band or of the gamma band. Degeneracies suggest symmetries and good quantum numbers and it was very recently demonstrated [12] that the arc of regularity in fact corresponds to the first example of a quasi-dynamic symmetry (QDS) within the triangle where all three symmetries are in play. (As pointed out by [13], earlier examples of QDS's were positioned along the legs of the triangle bridging only the two symmetries bounding the leg.) Thus it is interesting to look at  $E0$  transitions for a calculation corresponding to a point on the arc.

As can be seen, the  $E0$  strength is now considerably more spread out, with a number of new transitions appearing, especially for the higher lying levels. It is interesting to

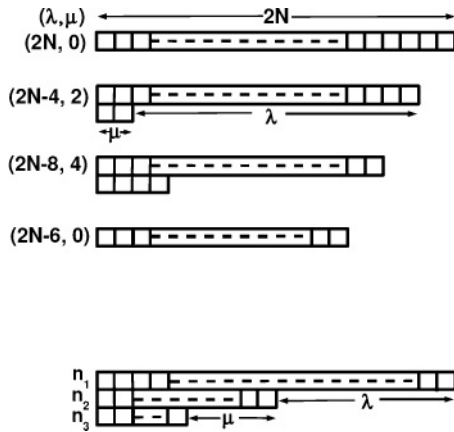


FIG. 4. Example of the determination of the  $(\lambda, \mu)$  quantum numbers of the  $SU(3)$  symmetry using the method of Young Tableaux [10,11].

compare this to a nucleus located close to the middle of the triangle but lying off the arc. The green dot in Fig. 1 corresponds to such a situation for which  $R_{4/2} \sim 3.1$ .

It is easy to see by inspection in Fig. 5 that the  $E0$  strength continues to spread. Further it is not only a question of more finite  $E0$  strengths but also many of these transitions are quite weak.

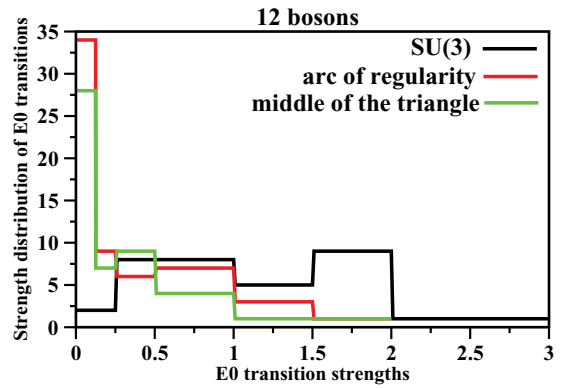


FIG. 6. (Color online) Distribution of the  $E0$  transition strengths for 12 bosons for  $SU(3)$ , for a point on the arc of regularity (red) and near the middle of the triangle (green). All values of the  $E0$  transitions between all  $0^+$  states are normalized to unity for the  $0_2^+ \rightarrow 0_1^+$   $E0$  transition strength.

An interesting way to look at these distributions is in terms of the histogram in Fig. 6 which shows the number of transitions in various strength bins for the three calculations. For this figure each calculation has been normalized so that the  $E0$  transition from the first excited  $0^+$  state to the ground state has a strength of unity. The  $SU(3)$  distribution is rather flat with very few weak transitions, that is, all allowed transitions

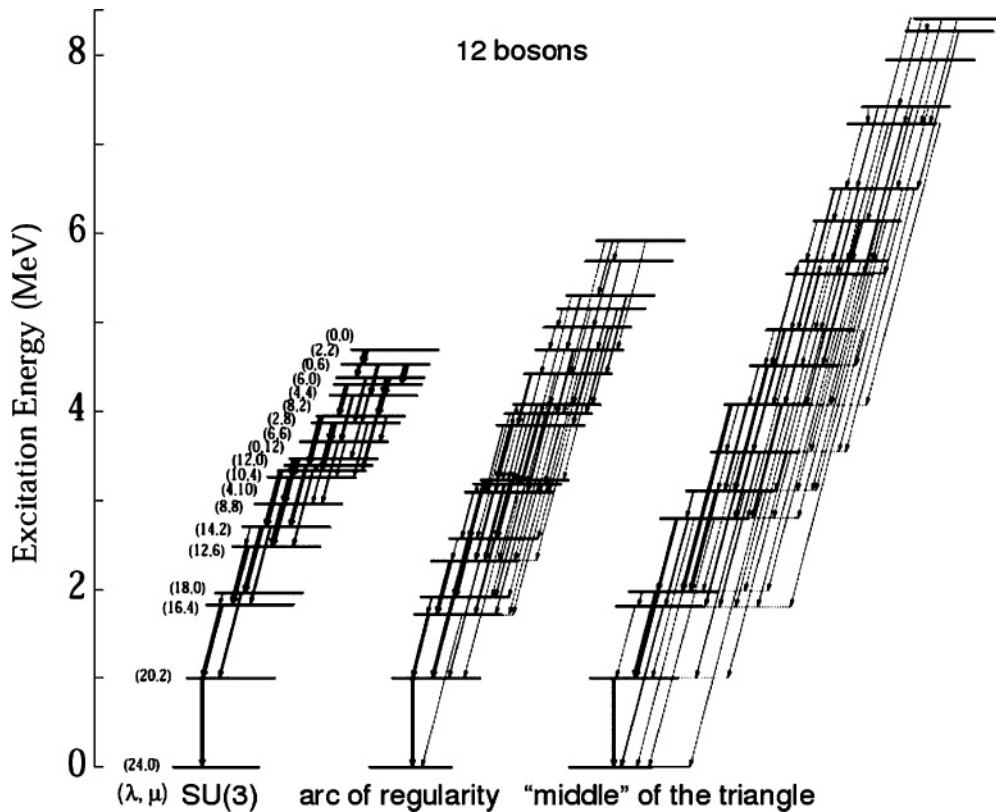


FIG. 5. Results for three calculations are shown for the case of  $N = 12$  bosons. Left: Typical spectrum of the  $0^+$  levels of the  $SU(3)$  limit labeled by their quantum numbers  $(\lambda, \mu)$  and the allowed  $E0$  transitions between all  $0^+$  states. Middle: Similar figure for  $E0$  transition strengths between all  $0^+$  levels corresponding to a point on the arc of regularity. Right: The  $E0$  transition strengths between all  $0^+$  levels corresponding to a point near the middle of the triangle.

have reasonably strong strengths. The distribution for the two calculations deviating from SU(3) clearly show many more weak transitions and a sapping of strength from the stronger transitions.

## V. CONCLUSIONS AND OUTLOOK

In this study, we calculated  $E0$  transitions between all  $0^+$  states using the IBA model to probe their relation to collectivity. For SU(3), we discovered a new selection rule that simultaneously describes all  $E0$  transitions. Although the spectrum of allowed  $E0$  transitions is complex we discussed

a very simple selection rule in terms of Young Tableaux with three rows. Finally, we studied the fractionation of  $E0$  strength between excited states for calculations deviating from the dynamical symmetries and noted the somewhat different patterns for nuclei along the arc of regularity and near the middle of the triangle.

## ACKNOWLEDGMENTS

We are grateful to F. Iachello, D. Bonatsos, and Y. Alhassid for useful discussions. Work supported by the US DOE under Grant No. DE-GF02-91ER40609.

- 
- [1] J. L. Wood, E. F. Zganjar, C. De Coster, and K. Heyde, *Nucl. Phys. A* **651**, 323 (1999).
  - [2] M. Sambataro and G. Molnar, *Nucl. Phys. A* **376**, 201 (1982).
  - [3] K. Heyde and R. A. Meyer, *Phys. Rev. C* **37**, 2170 (1988).
  - [4] J. Jolie, R. F. Casten, P. Cejnar, S. Heinze, E. A. McCutchan, and N. V. Zamfir, *Phys. Rev. Lett.* **93**, 132501 (2004).
  - [5] F. Iachello and A. Arima, *The Interacting Boson Model* (Cambridge University Press, Cambridge, 1987).
  - [6] J. Bonnet, A. Krugmann, J. Beller, N. Pietralla, and R. V. Jolos, *Phys. Rev. C* **79**, 034307 (2009).
  - [7] S. Zerguine, P. Van Isacker, A. Bouldjedri, and S. Heinze, *Phys. Rev. Lett.* **101**, 022502 (2008).
  - [8] K. Wimmer *et al.*, in *Proceedings of the 13th International Symposium on Capture Gamma-Ray Spectroscopy and Related Topics, Cologne, Germany* [AIP Conf. Proc. **1090**, 539 (2009)].
  - [9] Y. Alhassid and N. Whelan, *Phys. Rev. Lett.* **67**, 816 (1991).
  - [10] K. T. Hecht, *Collective Models*, Proceedings of the NUFFIC International Summer Course in Science at Nijenrode Castle, Netherlands (North-Holland Publishing Company, Amsterdam, 1964).
  - [11] R. F. Casten and D. D. Warner, *Rev. Mod. Phys.* **60**, 389 (1988).
  - [12] Dennis Bonatsos, E. A. McCutchan, and R. F. Casten, *Phys. Rev. Lett.* **104**, 022502 (2010).
  - [13] D. J. Rowe, M. J. Carvalho, and J. Repka, *Rev. Mod. Phys.* (in press, 2011).